Performance Enhancement of Poly(lactic acid) and Sugar Beet Pulp Composites by Improving Interfacial Adhesion and Penetration

Feng Chen,[†] LinShu Liu,*[,‡] Peter H. Cooke,[‡] Kevin B. Hicks,[‡] and Jinwen Zhang*[,†]

Materials Science Program & Wood Materials and Engineering Laboratory, Washington State University, Pullman, Washington 99164, and Eastern Regional Research Center, Agricultural Research Service, U.S. Department of Agriculture, 600 East Mermaid Lane, Wyndmoor, Pennsylvania 19038

Sugar beet pulp (SBP), the residue from the sugar extraction process, contains abundant dietary fibers and is mainly used for feedstuff. In this study, poly(lactic acid) (PLA) and SBP composites were prepared using a twin screw extruder. The phase structure, thermal properties, mechanical properties, and water absorption of the composites were studied. The molecular weight change of PLA in the composites was also studied. Polymeric diphenylmethane diisocyanate (pMDI) was used as a coupling agent and resulted in significant increases in mechanical properties and water resistance. The tensile strength of the PLA/SBP (70/30 w/w) composite was only 56.9% that of neat PLA, but it was increased to 80.3% with the addition of 0.5% pMDI and further increased to 93.8% at 2% pMDI. With 50% SBP and 2% pMDI, the tensile strength of the composite was 87.8% of that of neat PLA. The microstructure of the composites indicated that the addition of pMDI greatly improved the wettability of the SBP particles by PLA and increased the penetration of PLA into the porous SBP. Consequently, the failure of the composites in mechanical testing changed from extensive debonding without pMDI to progressive rupture of the SBP particles with pMDI.

Introduction

Poly(lactic acid) (PLA) is a commercially available biobased thermoplastic polymer using a renewable feedstock, corn starch. PLA offers a potential alternative to petrochemical plastics in many applications, in part because of its relatively high strength and stiffness.[1−3] However, the relatively high price, low heat distortion temperature (HDT), and low toughness are obstacles to a broad application of PLA. In recent years PLA composites with natural fibers have received extensive study. In addition to their cost effectiveness and light weight, natural fibers generally result in an increase in the modulus of PLA composites. On the other hand, the effectiveness of natural fibers to improve mechanical strength and impact properties of the products depends on the composite fabrication method, interfacial adhesion, fiber type, and reinforcement from the characteristics of the fiber, including diameter and average length/diameter ratio (L/D) of the specific fiber. PLA/lyocell fabric laminates showed overall improvement of tensile and impact properties with fabric content,[4] while in PLA laminates with randomly oriented hemp fibers the tensile and modulus reached maxima and then decreased with fiber content.[5] However, more reported studies were done with short natural fiber reinforced PLA composites prepared by melt compounding (i.e., extrusion) and injection molding. Short natural fibers, such as chopped hemp[6] and abaca fibers,[7] were shown to increase not only the tensile and flexural strengths of PLA composites but also the impact properties. Conversely, the low cost flour-type fibers, such as wood flour[8] and ground bamboo fiber,[9] showed little or even detrimental effect on the tensile strength of PLA composites and decreased the impact strength.[10] The different effects of short and flour-type natural fibers were most likely related to the large difference in their L/D ratios. The natural fibers in flour form usually have L/D ratios less than 10, while the chopped short fibers could have significantly higher L/D ratios (i.e., 50 or higher). It is well-known that stress transfer can only be developed effectively at a certain level of L/D ratio for short fiber/polymer composites.[11] Nevertheless, use of flour-type natural fibers has the advantage of better mixing and easier processing besides being more economical. Therefore, there is still great interest in utilizing those low cost cellulosic fillers for polymer composites.

The residue left by sugar extraction from beets, the sugar beet pulp (SBP), is composed of ca. 75% polysaccharides (cellulose, hemicellulose, pectin) and 25% others including protein, residual sugar, lignin, etc. The United States is the largest producer of sugar beets, and the sugar industry yields about 40 million tons of SBP.[12] Currently SBP is mainly used as an ingredient in animal feed or is simply disposed of as solid waste. Cellulose microfibers and nanofibers isolated from SBP have been reported in the literature[13,14] and used to prepare polymer composites.[15] Recently we studied the utilization of the whole SBP as a filler in PLA composites.[16−18] Compared with neat polymer samples, compression-molded composite samples demonstrated drastic deterioration in strength and increasing brittleness as the SBP content increased, probably owing to the severe thermal degradation of PLA at high molding temperatures (200 °C). Although the injection-molded composite samples showed improved mechanical properties with respect to the compression-molded samples, without fiber surface treatment or addition of compatibilizer, the resulting composites still showed great deterioration in strength as the SBP content increased.[17] Adding sorbitol and glycerol as plasticizers improved the ductility, but resulted in a further decrease in the tensile strength of the composites.[18] The extensive debonding observed in the scanning electron micrographs of the fracture surfaces suggested a poor interfacial adhesion between the PLA matrix and SBP.

It was found that the pulp still retains the biological cell structure[14] after sugar is extracted from beets.[19] Therefore, if the matrix polymer can effectively penetrate SBP particles and fill the pores by improving the wetting of the SBP particles,

* To whom correspondence should be addressed. Tel.: (509) 335-8723(J.Z.); (215) 233-6486(L.L.). E-mail: jwzhang@wsu.edu (J.Z.); LinShu.Liu@ars.usda.gov (L.L.).
[†] Washington State University.
[‡] U.S. Department of Agriculture.

10.1021/ie800930j CCC: $40.75
Published on Web 10/28/2008

high mechanical strength of the composites can be expected because of both the strong interfacial bonding and good mechanical interlocking. Studies have indicated that strength of the PLA composites with both short natural fibers and flour-type natural fibers can be greatly increased by improving interfacial adhesion through fiber surface modification[7,8] or by using isocyanate-type coupling agents.[9] Because of its low volatility and easy penetration of wood, polymeric diphenylmethane diisocyanate (pMDI) has long been used as a cold-setting adhesive in the wood composite industry.[20] In recent years pMDI and other isocyanates have found uses as coupling agents in thermoplastic polymer and natural fiber composites,[21] and have been shown to be more efficient coupling agents than maleic anhydride grafted copolymers.[22] Isocyanates have also been used as coupling agents for the compatibilization of binary PLA blends with other eco-friendly polymers[23,24] or starch,[25] where coupling reactions between the polymers were noted to take place at the interfaces.[23−25]

The objective of this study was to improve the mechanical properties of PLA/SBP composites through improving the interfacial interaction using pMDI as a coupling reagent. Composites with and without pMDI were melt-compounded using a twin screw extruder, and the test specimens were injection-molded. The change of PLA molecular weight after processing was measured. Tensile, impact, and thermal properties were studied. The phase structure and microstructure of fracture surfaces of the composites were examined using scanning electron microscopy (SEM) and confocal scanning microscopy. The water absorption and wet strength were also measured.

Experimental Section

Materials. PLA was obtained from NatureWorks (Minnetonka, MN), and the pellets were ground into powder with an average particle size of ca. 300 μm by a mill in the presence of dry ice. The weight-average molecular weight of PLA was 135 kDa with a polydispersity index of 1.38. SBP with an average particle size of ca. 30 μm was provided by Danisco (New Century, KS) and used as received. Per the manufacturer, it composed of ca. 73 g of dietary fiber (29 g of hemicellulose, 22 g of pectin, 18 g of cellulose, 4 g of lignin), 10 g of protein, 4 g of sugar, 4 g of minerals, and 0.5 g of fat on the basis of 100 g of SBP. pMDI (Mondur 541) was a viscous liquid obtained from Bayer MaterialScience LLC (Pittsburgh, PA) and contained 31.5 wt % NCO.

Composite Preparation. A co-rotating twin screw extruder (Leistritz ZSE-18) equipped with a volumetric feeder and a strand pelletizer was employed to compound the PLA/SBP composites. The extruder had a screw diameter of 17.8 mm and an L/D ratio of 40, with eight controlled temperature zones which were set to range from 150 °C (next to the feeding segment) to 170 °C (die adaptor). The screw speed was maintained at 100 rpm for all runs. Before extrusion, PLA powder was dried at 98 °C in a convection oven for 16 h. SBP was dried in a vacuum oven at 4 mmHg and 70 °C for 8 h. The residual moisture content in SBP was found to be ca. 0.88 wt % by drying the sample to constant weight in a conventional oven at 105 °C. PLA and SBP were manually premixed by tumbling in a plastic zip-lock bag. A small portion of this mixture was first thoroughly mixed with the required amount of pMDI in a kitchen blender; then the rest of the mixture was added and mixed for about 1 min. The extrusion compounding was followed right after premixing of the materials. The extrudate was cooled in a water bath and subsequently pelletized. Standard tensile test specimens (ASTM D638, type I) were prepared by injection molding (Sumitomo SE 50D). The injection molding zone temperatures from feed zone to nozzle were set at 165, 170, 170, and 170 °C, respectively. Prior to injection molding, the pellets prepared from the extrusion were dried in a convection oven at 98 °C for 16 h.

Molecular Weight Measurement. PLA molecular weight was measured before and after extrusion by gel permeation chromatography (GPC) as described previously.[16] Chloroform was the solvent used for extracting PLA from the injection-molded composites. The composite sample was placed in $CHCl_3$ at room temperature for ca. 8 h, and then the filtrate was collected. The polymers dissolved in $CHCl_3$ were precipitated with acetone. Because $CHCl_3$ was not a solvent for the SBP ingredients (pectin, cellulose, hemicellulose, etc.) and their coupling products with PLA, the extracted polymers were assumed to be only PLA and chain-extended PLA. GPC measurements were carried out on a Shimadzu HPLC system (LC-10AD, Kyoto, Japan) equipped with a Phenogel guard column (22824G, 50 mm × 7.8 mm), a Phenogel column (GP/4446, 300 mm × 7.8 mm; Phenomenex, Torrace, CA), a refractive index detector (RID 10A), and an SCL-10A data station. Tetrahydrofuran (THF) was used as a mobile phase at the flow rate of 1 mL/min. The molecular weight of PLA was determined against a universal calibration that was prepared by the use of a set of polystyrene standards.

Mechanical Testing. All test specimens were conditioned for 7 days at 23 °C and 50% relative humidity prior to testing. Tensile tests were performed on an 8.9-kN, screw-driven universal testing machine (Instron 4466) equipped with a 10-kN electronic load cell and mechanical grips. The testing was conducted following ASTM D638 at a crosshead speed of 5 mm/min with deformations measured using a 25-mm extensometer (MTS 634.12E-24) and data acquired by computer. Five replicates were tested for each sample to obtain an average value.

Notched Izod impact tests were performed according to ASTM D256 method C on a plastic impact tester (Tinius Olsen). The flexural test samples were cut into halves, and the halves far from the gate (far end) were used for the impact testing. All samples were notched according to the ASTM standard using a cutter with a tip radius of 0.25 mm.

Thermal Analysis. Differential scanning calorimetry (DSC) was performed on the injection-molded specimens. The samples were crimp sealed in 40-μL aluminum crucibles. All samples were first scanned from 25 to 180 °C at the heating rate of 10 °C/min to examine the glass transition temperature and crystallinity of PLA in the test specimens. The samples were isothermally kept at 180 °C for 2 min and then cooled to 25 °C at 10 °C/min to study the non-isothermal melt crystallization.

Microscopic Analysis. Scanning electron microscopy (SEM) (Hitachi S-570) and confocal laser scanning microscopy (CLSM) were used to examine the morphological structures of the composites and the topography of the fracture surfaces. For the SEM experiments, all specimens were sputter coated with gold for 8 min prior to examination. CLSM images were obtained by confocal fluorescence for SBP (excitation/emission, 488/500−530 nm) and confocal reflection for PLA (488 nm) in two separate channels using an IRBE optical microscope with a 20× lens integrated with a Model TCS-SP laser scanning confocal microscope (Leica Microsystems, Exton, PA). The distribution of SBP and PLA was visualized in sets of optical sections extending from the surface to deep (~30 μm) within the composite.The size distribution of SBP in digital images of fracture surfaces with and without pMDI was analyzed from

Table 1. Effect of Processing on the Molecular Weights of Neat PLA and PLA in the Composites

PLA composites	% pMDI	M_w	M_n	M_w/M_n
PLA[a]	N/A	135 000	98 000	1.38
PLA[b]	0	125 000	85 000	1.47
PLA[b]	2.0	145 000	105 200	1.38
PLA/SBP[c]	0	97 500	65 000	1.50
PLA/SBP[c]	0.5	98 200	65 500	1.50
PLA/SBP[c]	1.0	95 000	70 400	1.35
PLA/SBP[c]	2.0	92 500	64 000	1.45
PLA/SBP[c]	3.0	100 800	70 500	1.43

[a] Unprocessed PLA. [b] Experienced the same extrusion and injection molding process as the composites. [c] The ratio of PLA:SBP in the composite is 70:30 (w/w).

images collected with an MZFl3 stereofluorescence microscope (Leica Microsystems, Bannockburn, IL). Matching areas of image frames from two samples were cropped and analyzed by digital image analysis using Fovea 3.0 plug-ins (Reindeer Graphics, Asheville, NC) for Adobe PhotoShop 7.0 (San Jose, CA). Color digital images of the autofluorescence from SBP were converted to monochrome (gray) images and calibrated to micrometers. The "surface" was flattened before setting gray level thresholds to define the bright (fluorescent) SBP particles by visually matching the thresholds by eye, before computing the particle size distributions as equivalent diameters. The results were incorporated as text files into spreadsheets and compared graphically in histograms.

Water Absorption. A water absorption test was conducted following ASTM D570-81 with a slight modification. The samples were conditioned for 7 days at 23 °C and 50% relative humidity prior to testing and then immersed in distilled water at room temperature. The percentage weight gain was taken as the water absorption value. Five replicates were tested for each sample.

Statistical Analysis. Results of tensile mechanical properties were analyzed by one-way analysis of variance (ANOVA) and the Tukey test under 95% confidence level ($\alpha = 0.05$) using the SAS/STAT software package.

Results and Discussion

Molecular Weight Changes of PLA. GPC was used to analyze the molecular weight change of PLA in the injection-molded PLA and PLA/SBP test specimens. PLA is sensitive to thermal degradation[26] and hydrolysis.[2,27] Decreases in PLA molecular weight were anticipated after melt processing, and it could be further reduced due to the residual moisture in SBP. As shown in Table 1, the melt processing caused a decrease in the PLA molecular weight, and it was likely due to thermal degradation under the processing conditions. The molecular weight of PLA in the composites showed an even larger decrease, and this could be attributed to a combined effect of PLA hydrolysis and thermal degradation. The complex ingredients in SBP, e.g., pectin, which contains a large number of carboxylic acid groups, might also cause or accelerate the above PLA degradation processes. Interestingly, adding 2% pMDI resulted in a 16% increase in the molecular weight of the neat PLA. This result suggests that pMDI caused the chain extension of PLA by cross-linking the terminal hydroxyl groups in PLA. A similar result using hexamethylene diisocyanate as a chain extender for PLA was reported elsewhere.[28] The increase in molecular weight by coupling reactions was also noted in the PLA/poly(butylene succinate) blends.[23] On the other hand, the molecular weight of PLA in the composites did not show a significant change with the addition of pMDI, suggesting that

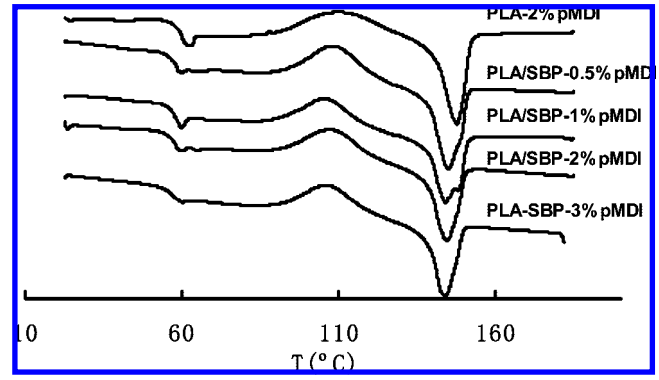

Figure 1. DSC thermograms of PLA and PLA/SBP (70/30) composites (first scan).

the PLA chain extension reaction in the composite might not be as effective as it was in neat PLA. The isocyanate group in PMDI is an active cross-linker that reacts with nucleophiles, such as hydroxyl groups, amino groups, and carboxyl groups, to form stable urethane, urea, or other linkages. Since all the major ingredients in SBP contain abundant hydroxyl and other functional groups which can react with pMDI, the extensive coupling reactions between pMDI and the SBP ingredients could be anticipated. Because the coupled PLA/SBP polymers were not able to dissolve in the THF solvent, their influence on the change of PLA molecular weight was not explored. Compared with the concentration of functional groups in SBP, the concentration of terminal hydroxyl groups in PLA is insignificant. Therefore, the reaction between SBP and pMDI was reasonably believed to be dominant, while the chain extension of PLA in the composite system was minor. As a result, the molecular weight of PLA in the composite showed little change with the addition of pMDI. In addition, the residual moisture in SBP would easily react with pMDI. Bao et al. noted the urea structure presented in wood composite using pMDI as adhesive, which resulted from the reaction of isocyanate with the residual water.[29] When the moisture content is low, pMDI reacts with the −NH− of urea to form an interpenetrating network of polyurea and biuret within the woody material.

Thermal Properties. Figure 1 shows the DSC thermograms of injection-molded PLA and its SBP composite samples. The results from the first heat scan revealed the glass transition and crystalline status of the PLA component in the injection-molded test specimens. The summary of the DSC results is given in Table 2. Although the PLA used was semicrystalline, it did not present significant crystallization in the injection-molded samples. This result was consistent with the conclusions in our previous study of PLA and its composites.[1−3] Cold crystallization was observed for the neat PLA and each of its composites. The very similar ΔH_{cc} and ΔH_m values in both neat PLA and composites suggest that the PLA was primarily amorphous in the injection-molded specimens. This was probably due to a quenching effect from the rapid cooling of the melt in the mold so that PLA was not able to crystallize during the molding process. The very small enthalpy of melt crystallization at a cooling rate of 10 °C/min supported this view (Table 2). The presence of SBP seemed to slightly increase the melt crystallization (increased T_{mc} and ΔH_{mc}), likely owing to the heteronucleation and growth of PLA crystals on the surface of the SBP. Furthermore, SBP also increased the cold crystallization of PLA (reduced T_{cc} and increased ΔH_{cc}). Conversely, the melting temperature of PLA was suppressed in the presence of SBP, probably due to the inhomogeneous crystallites. The effect of pMDI on the crystallization of PLA in the composites was not clear. The fluctuation

Table 2. DSC Results of Neat PLA and Its SBP Composites[a]

composition			cold[b] crystallization		melting[b]		melt crystallization	
PLA/SBP	pMDI (%)	T_g[b] (°C)	T_{cc} (°C)	ΔH_{cc}[c] (J/g)	T_m (°C)	ΔH_m[c] (J/g)	T_{mc} (°C)	ΔH_{mc}[c] (J/g)
100/0	0	57.8	112.3	19.1	148.5	−19.8 (0.7)	128.5	0.3
100/0	2	57.1	109.8	14.6	147.7	−19.7 (5.1)	129.3	0.8
70/30	0	55.7	109.2	22.3	145	−24.7 (1.4)	131.3	1.1
70/30	0.5	56.1	108.5	22.7	145	−28.4 (5.7)	131.5	1.0
70/30	1	56.1	105.8	21.4	144.2	−23.4 (2.0)	130.5	1.3
70/30	2	56.2	109.2	19.4	145	−25.1 (5.7)	130.3	1.5
70/30	3	55.3	106.3	20.9	144	−21.9 (1.0)	124.3	0.9

[a] Results are the average of two repeats. [b] Results from the first heating scan. [c] Data corrected for the percentage of PLA in the composite.

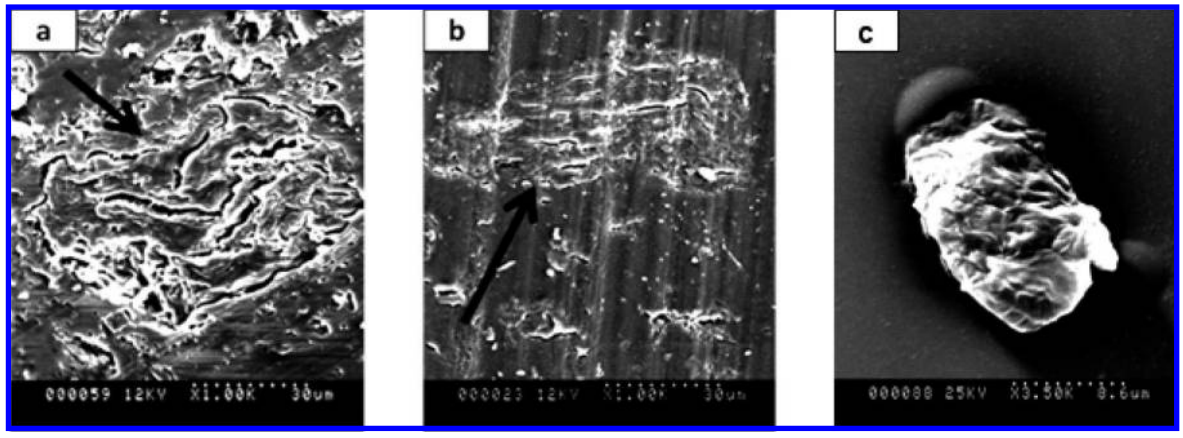

Figure 2. Representative SEM micrographs showing SBP articles in the PLA/SBP (70/30 w/w) composites without pMDI (a) and with 2% pMDI (b). The flat surfaces were cut using an ultramicrotome under liquid nitrogen cooling. The intact SBP particles (c) are also shown here.

Table 3. Effect of pMDI on Tensile Properties of Neat PLA and PLA/SBP Composites

composition		dry test					wet test after 4-day immersion				
			modulus (GPa)		elongation (%)			modulus (GPa)		elongation (%)	
PLA/SBP	pMDI (%)	strength (MPa)					strength (MPa)				
100/0	0	65.5 ± 0.4	3.8 ± 0.2	A[a]	3.6 ± 0.4	A[a]	62.6 ± 0.1	3.7 ± 0.1	AB[a]	4.7 ± 0.1	A[a]
100/0	**2**	**64.0 ± 0.3**	**3.6 ± 0.2**	**A**	**3.5 ± 0.5**	**A**	**63.9 ± 0.9**	**3.5 ± 0.1**	**A**	**5.1 ± 1.1**	A
70/30	0	37.3 ± 0.2	4.8 ± 0.1	B	2.3 ± 0.3	CD	34.7 ± 0.5	3.9 ± 0.1	BC	2.7 ± 0.4	B
70/30	**0.5**	**52.6 ± 0.4**	**4.7 ± 0.2**	**B**	**1.8 ± 0.1**	**D**	**49.4 ± 0.2**	**4.1 ± 0.1**	**CD**	**2.2 ± 0.3**	B
70/30	1	55.6 ± 0.4	4.7 ± 0.1	B	2.4 ± 0.2	BC	52.2 ± 0.2	4.2 ± 0.1	D	3.1 ± 0.1	B
70/30	**2**	**61.1 ± 0.7**	**5.0 ± 0.2**	**B**	**2.8 ±0.3**	**AB**	**53.8 ± 0.7**	**4.2 ± 0.1**	**D**	**2.8 ± 0.3**	**B**
70/30	3	58.7 ± 0.5	4.7 ± 0.1	B	2.9 ± 0.2	A	56.3 ± 0.3	4.3 ± 0.2	D	4.2 ± 0.2	A

[a] One-way ANOVA analysis (SAS) and Tukey multiple comparison of the effects of SBP and pMDI. Values with different letters mean they are significantly different from each other. The confidence level was set at 95%.

of the enthalpy of PLA crystallization (cold and melt) and of the heat of PLA fusion from composite to composite was probably due to the variation of the exact amount of PLA in the particular sampling.[2,3,30] Only at 3% pMDI did the melt crystallization ability of PLA show an apparent decrease as shown in the reduction of T_{mc}. It is interesting to note that the T_g of composites showed a slight decrease with respect to that of neat PLA. Similar thermal properties of the PLA/SBP composites were also recently reported by Mohamed et al.[31]

Morphology of the Composites. The improved interfacial adhesion by the addition of pMDI can also be noted by the change in the wetting of SBP particles by the PLA matrix in the composites (Figure 2). Considering that the stress involved in the usual cryofracturing preparation of SEM sections might cause the debonding of the fillers, particularly for the uncompatibilized samples, in this study the flat SEM sections in Figure 2 were cut using a Powertome X (Boeckeler Instrument) cryo-ultramicrotome on the untested specimens. A flat surface prepared this way would maximally retain the phase structure in its original state. Figure 2a shows the phase structure of the PLA/SBP (70/30 w/w) without pMDI; a section of a SBP particle is presented in the micrograph. The hollow areas in the particle were attributed to the porous structure of SBP. There also existed some interstices between the particle and matrix. Similar interstices were also observed in PP/bamboo fiber,[32] PHBV/flax,[33] and PP/wood flour[34] composites in the absence of interfacial adhesion promoters. These observations suggest that the wettability of SBP articles by PLA was poor in the absence of pMDI, and the polymer was not able to effectively penetrate the particles. With 2% pMDI added (Figure 2b), however, the pores of the SBP particles were better filled with PLA, and the interstices between the particle and matrix became less, suggesting that better wetting was achieved. As mentioned previously, the extensive coupling reactions between pMDI and SBP turned the hydrophilic surface of SBP particles hydrophobic and resulted in enhanced interfacial adhesion and PLA penetration. In addition, the coupling reactions between PLA and SBP also contributed to the improved interactions between the two phases. The difference in phase structures between the composite without pMDI and the composite with pMDI largely accounted for the difference in their mechanical properties. The former had weak interfacial adhesion and was susceptible to debonding

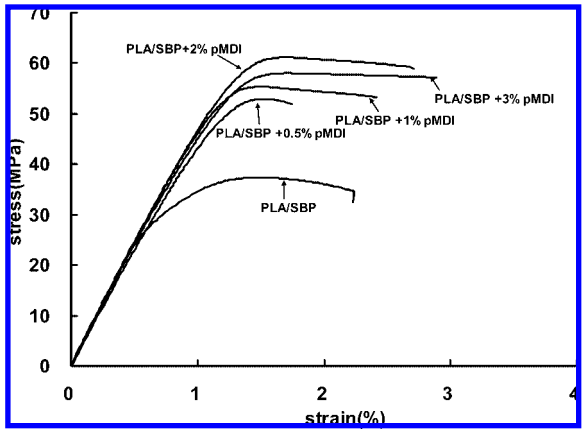

Figure 3. Stress−strain curves showing the effect of pMDI on tensile properties.

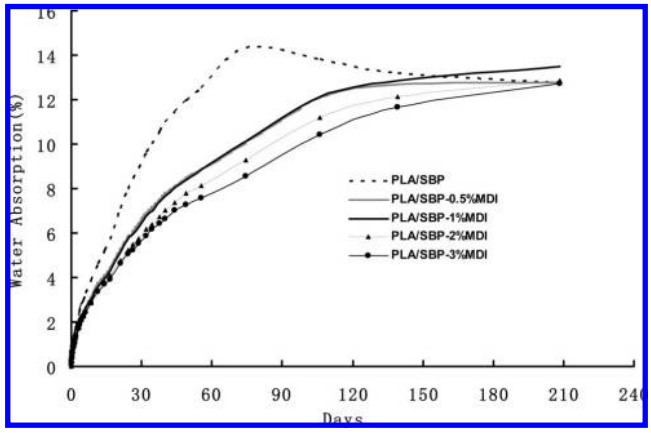

Figure 4. Effect of pMDI on water sorption of PLA/SBP (70/30 w/w) composites.

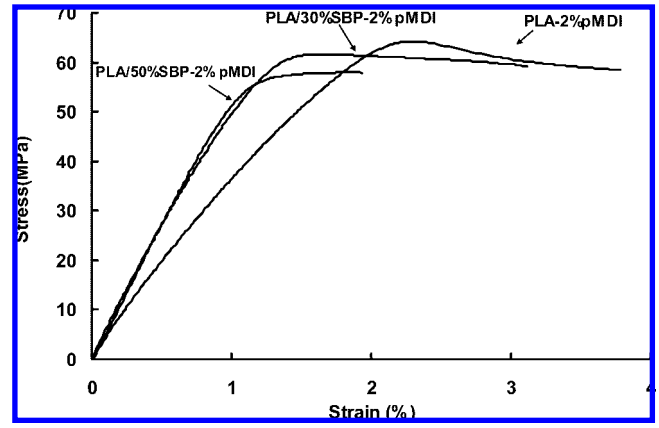

Figure 5. Comparison of composites with different SBP contents.

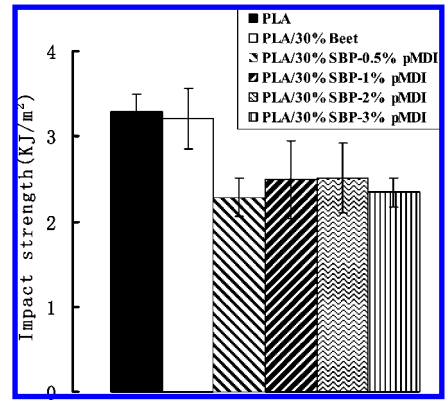

Figure 6. Effect of pMDI on impact strength of PLA/SBP (70/30 w/w) composites.

and hence resulted in lower yield stresses, and the latter possessed strong interfacial bonding force and better mechanical interlocking and hence yielded at higher stress. Detailed discussion of mechanical properties and fracture behaviors are described in the following sections.

Mechanical Properties and Water Resistance. Table 3 summarizes the tensile properties of PLA and its SBP (70/30 w/w) composites. One-way ANOVA statistical analysis was applied to evaluate the data under the 95% confidence level. Examination of the *p*-value of every property showed that the addition of SBP and the pMDI concentration significantly affected the strength, modulus, and percentage elongation of the composites. Tukey multiple comparison further identified the significant differences among the seven samples at $\alpha = 0.05$. The samples which had the same labeling letter were not significantly different from each other. For example, in the dry test, PLA and PLA with 2% pMDI showed very similar moduli which were significantly different from that of the composites. The modulus of the composite was not statistically varied by the addition of pMDI. Compared to the neat PLA, the addition of 30% SBP in the composite resulted in ca. 26% increase in modulus of the material but drastically reduced the yield strength and the elongation as well. However, by adding only 0.5% pMDI, a large portion of the lost tensile strength was recovered. All samples showed significantly different strengths from each other.

Figure 3 shows the tensile stress−strain curves of PLA/SBP (70/30 w/w) composites with the pMDI content ranging from 0 to 3%. The tensile strength of the PLA/SBP (70/30 w/w) composite was only 56.9% that of neat PLA, but it was increased to 80.3% with the addition of 0.5% pMDI and further increased to 93.8% at 2% pMDI. SBP is highly hydrophilic, while PLA is very hydrophobic. There was a lack of strong interfacial adhesion between PLA and SBP as shown in Figure 2a. In a polymer/rigid particle system where interfacial adhesion is not high, debonding could occur at a lower tensile stress than the yield stress of the neat polymer.[3,35,36] This was also the case for the PLA/SBP composite without pMDI. Furthermore, the large amount of SBP tended to form agglomerates which triggered early fracture, resulting in a lower strain at break. pMDI proved to be an effective coupling agent in improving the compatibility of the two phases, resulting in an increase in tensile strength. As shown in Figure 2b, with the addition of 2% pMDI, PLA not only displayed a good wetting of the outer surface but also better diffused into the pores of SBP particles. In other words, the addition of pMDI promoted the formation of better mechanical interlocks between the filler and matrix. It was noted that the elongation showed a continuous increase with pMDI from 0.5 to 3% (Table 3), as is shown in the statistical analysis; with the addition of 3% pMDI, the strain at break is significantly different from that of the control sample without pMDI and is similar to that of the neat PLA. While increasing pMDI concentration tended to complete the reaction of the −CNO groups of pMDI with the hydroxyl groups at the surfaces of the porous SBP particles, it would also promote the reaction of −CNO with the residual water in SBP, forming the amine or urea compound which plasticized the composites. The fact that with 3% pMDI the composite showed a decrease in strength but a further increase in elongation supports such a mechanism. However, the modulus of the composites showed little change

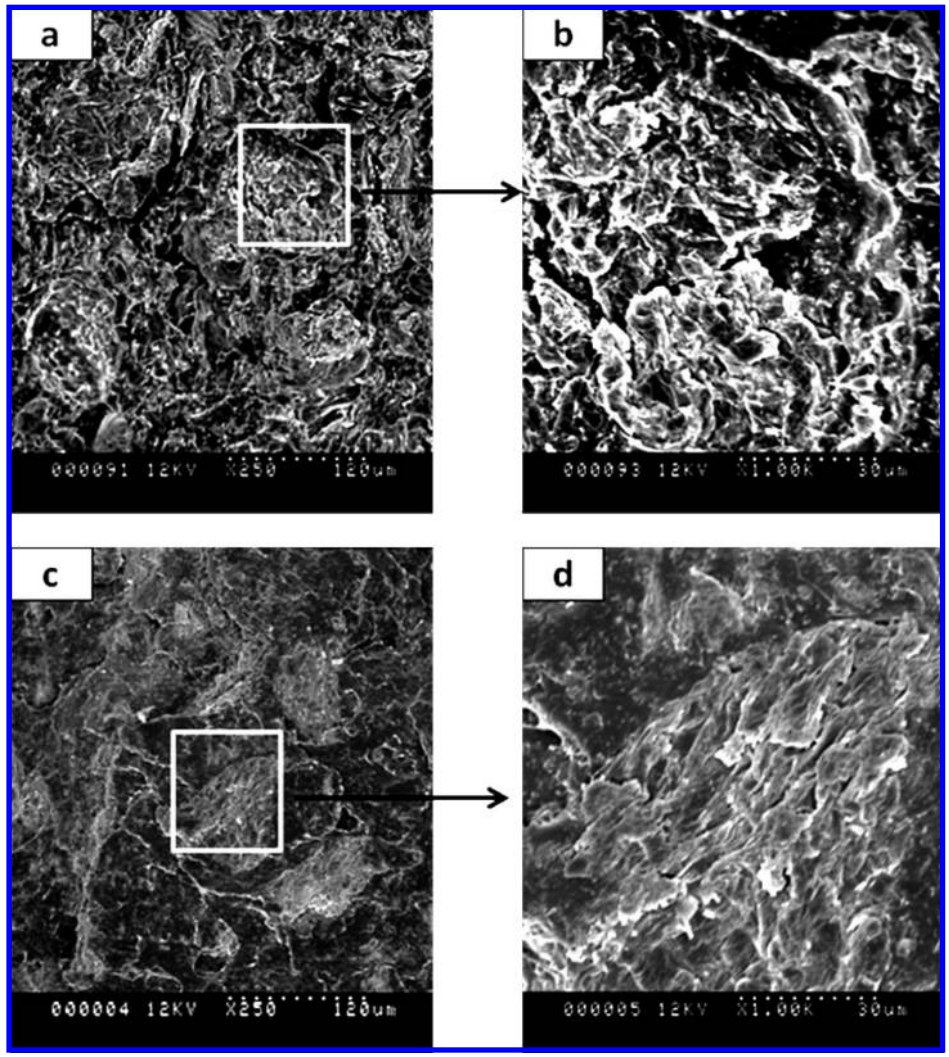

Figure 7. Representative SEM micrographs of impact fracture surfaces of PLA/SBP (70/30 w/w) composites. (a) 0% pMDI; (b) 2% pMDI.

with pMDI. Similar results were reported for starch/PLA blends where starch granules dispersed in the matrix and tensile strength increased with pMDI varying from 0 to 2%.[37] Similarly, the study of lap-shear strength of Aspen strands uniformly coated with pMDI resin suggested that the bonding of the dry strands became weak as the amount of pMDI resin increased.[38] It should be mentioned that our selective repeats of compounding experiments and subsequent molding of the composites with 0.5 and 3.0% pMDI yielded almost identical mechanical properties, suggesting good reproducibility of the results.

Figure 4 shows the water absorption of the PLA/SBP (70/30 w/w) composites with immersion time. It is obvious that the improved wetting of SBP by matrix with the addition of pMDI also led to the increase in water resistance. The water uptake continuously decreased with pMDI ranging from 0 to 3%. The water absorption of the composite without compatibilizer reached equilibrium at ca. 74 days, and then showed a decrease with further immersion, which was probably due to the loss of the ingredients of SBP into the water. The water absorption of the composites with 0.5% pMDI reached equilibrium after ca. 120 days, but water absorption of those with higher pMDI concentration had not reached equilibrium even after 200 days immersion in water. The slowed water absorption process by using pMDI appeared to be an advantage in terms of the wet strength. For example, after immersion in water for 4 days the average water uptake was ca. 2% for those compatibilized composites, and the composites largely retained their original high strength and stiffness (Table 3).

Figure 5 shows the effect of SBP content on the tensile properties of the composites. PLA exhibited yielding with a short quasi constant stress regime, and failed at ca. 3.5% strain. While the modulus of the composites increased with the SBP content, yield stress and elongation decreased accordingly. The yield stress of the composites with 30 and 50% SBP was 93.8 and 87.8% of the neat PLA, respectively. The change of modulus with the SBP content could be attributed to the additive nature of modulus of a composite as typically described in the role of a mixture (not analyzed in this study). The continuous decrease in yield strength and strain at break with the SBP content might suggest the early failure caused by the presence of large agglomerates. However, the high retention of strength in the composite with 50% SBP suggests that SBP could be used as a very competitive filler to other cellulosic fillers. A composite with 70% SBP was also attempted, but it had poor melt flowability with the present formulation and could not be properly injection-molded into test specimens.

Figure 6 gives the comparison of impact strength of PLA and its SBP composites. The PLA/SBP (70/30) composite demonstrated a very similar low impact strength comparable to the neat PLA. Addition of 0.5% pMDI resulted in an approximate 29% decrease in impact strength, but further increasing pMDI did not show significant effects. Like other

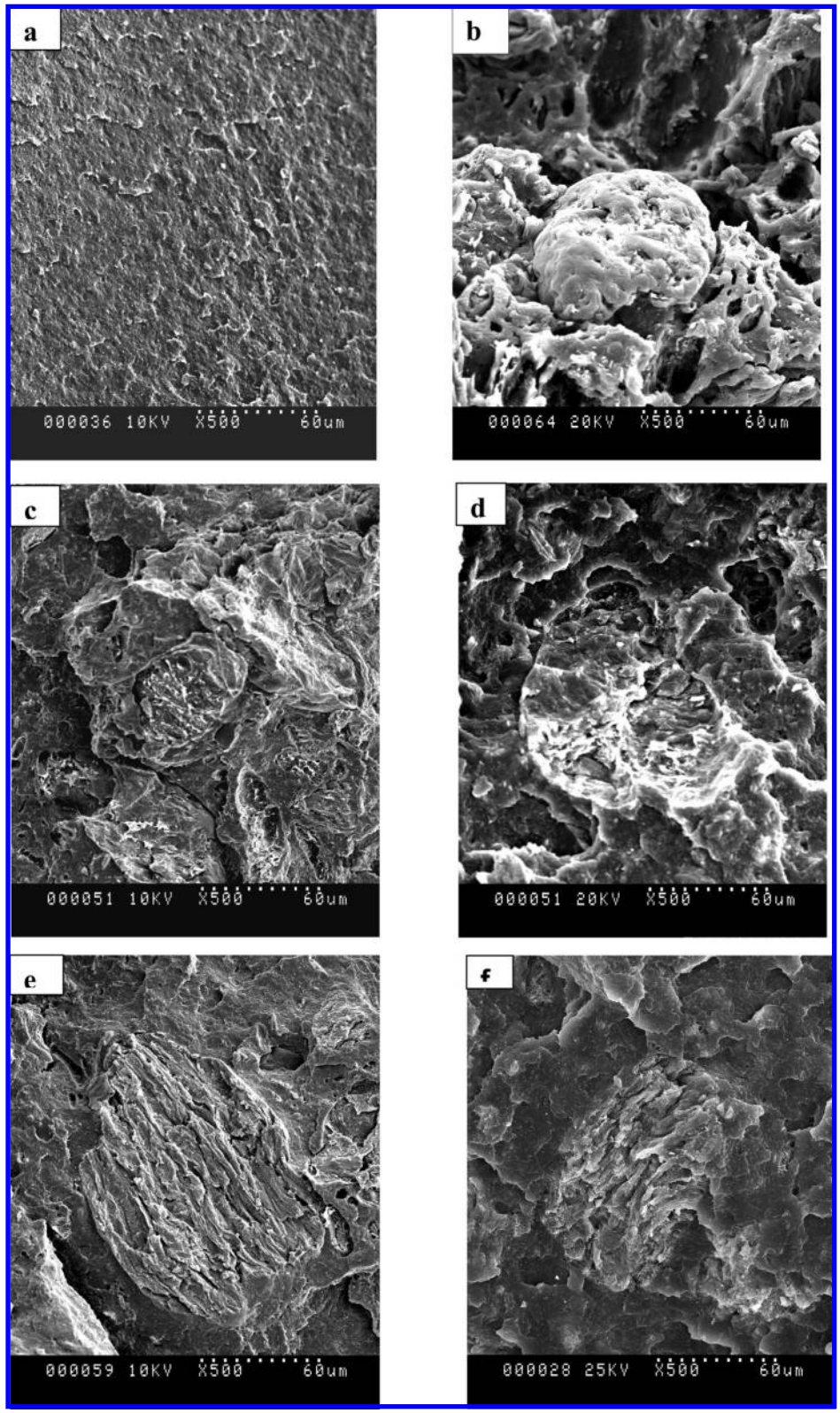

Figure 8. SEM micrographs of neat PLA (a) and PLA/SBP (70/30 w/w) composite with 0% (b), 0.5% (c), 1% (d), 2% (e), and 3% (f) pMDI, respectively.

methods for the measurement of toughness, impact testing also detects the energy consumed for the creation of fractures. Although the improved interfacial adhesion increased the tensile strength, it decreased the debonding of SBP particles from the PLA matrix, therefore reducing the energy consumption in creating new fracture surfaces.[11] Consequently, the impact strength was decreased. Figure 7 shows the SEM micrographs of the impact fracture surfaces of the composites. The rough surface reveals either the convex surface of SBP or the concave imprints left, suggesting that overwhelming debonding occurred in the composite without pMDI (Figure 7a). In contrast, the composite with 2% pMDI showed quite different impact fracture surfaces. There were rarely traces of the particle pullout; instead the SBP particles were extensively fractured along the same

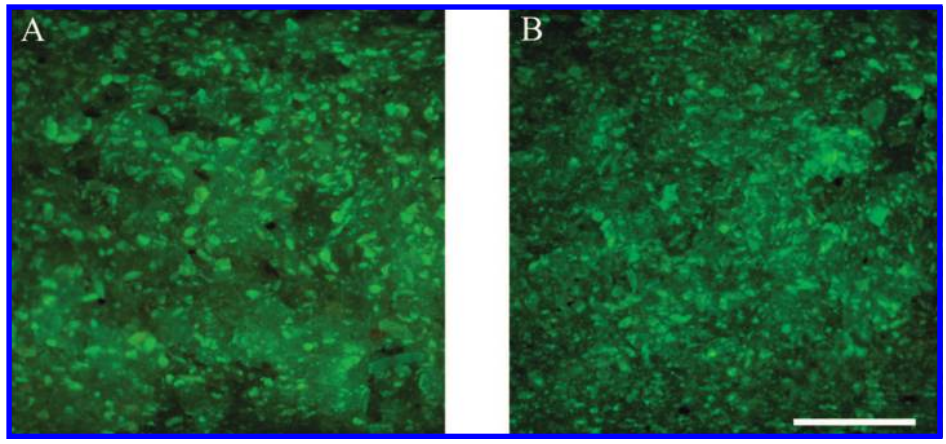

Figure 9. Stereofluorescence images of the fracture plane of the composites after tensile testing. (A) Green fluorescent SBPs distributed in PLA matrix without pMDI and (B) distribution of smaller fluorescent SBPs with pMDI. Scale bar is 1 mm.

plane as the fracture surface through the PLA matrix. The progressive change from pullout to fracture of the SBP particles with pMDI content is further elaborated in the section Morphology of Tensile Fracture Surfaces.

Morphology of Tensile Fracture Surfaces. The tensile fracture surfaces of PLA and its SBP composites after tensile testing were examined by SEM. Neat PLA showed a smooth fractured surface (Figure 8a), indicating a lack of significant plastic deformation, which corresponds to its low ductility. The rough fracture surface of the PLA/SBP (70/30 w/w) composite (Figure 8c,d) clearly showed the convex pullout SBP particles and the concave imprints left by the pullout SBP particles, indicating that the fracture of the composite occurred or started on the surfaces of SBP particles as a result of weak interfacial adhesion. With 0.5% pMDI added, in addition to debonding, fracture extending through the SBP particles was also noted (Figure 8c). With increasing addition of pMDI, there was less evidence of debonding observed at the fracture surfaces; instead, more breakup of the SBP particles on the fracture surface was noted (Figure 8e,f). The wettability of the SBP particles by the PLA matrix was apparently increased with the addition of pMDI so that the SBP particles were ruptured at the plane of the fracture surfaces. These SEM micrographs provide clear evidence that strong interfacial adhesion was established by the addition of pMDI.

Differences in the topography and microstructure of the fracture surfaces of composites with and without pMDI were also apparent by confocal fluorescence microscopy (micrographs not shown). The rupture of the SBP particles in the fracture plane of the composite with pMDI was also supported by an analysis of the distribution of particle sizes based on SBP fluorescence. The observed differences in the fracture surfaces with and without pMDI seen in SEM images suggested that the size distribution of the SBP particles should be different. If the fracture plane propagated around the interfaces because of the debonding in the absence of pMDI, then the area of SBP particles should be larger than when fractures propagated through the SBP particles in the presence of pMDI. To obtain evidence of this difference, the size distributions of fluorescent particles corresponding to SBP were collected by fluorescence microscopy (Figure 9) and measured by digital image analysis.

A comparison of equivalent diameters is plotted as histograms in Figure 10. The average (equivalent) diameters of SBP particles with and without pMDI were found to be 20.2 and 28.3 μm, respectively. Fewer SBP particles with pMDI were found at each size class plotted. Without pMDI, the percentage

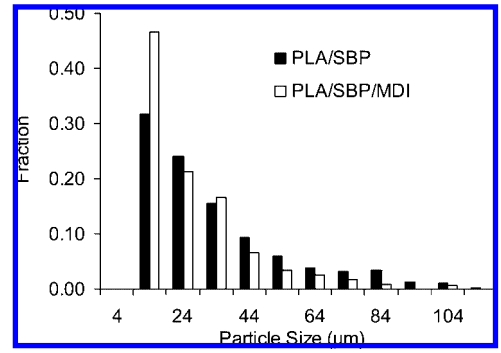

Figure 10. Size distribution of SBP particles in PLA matrix with and without MDI.

of particles with diameters greater than 40 μm was greater than with pMDI, suggesting that the fracture plane defines the circumference of whole SBP particles because of debonding from the PLA in the absence of pMDI.

Conclusions

PLA/SBP composites with improved tensile mechanical properties were successfully prepared by extrusion compounding. pMDI was an effective coupling agent which greatly improved the tensile strength of the resulting composites. As the pMDI concentration gradually increased from 0.5 to 2%, tensile strengths of the PLA/SBP (70/30 w/w) composites increased and approached that of neat PLA. With 50% SBP and 2% pMDI, the tensile strength of the composite was 87.8% of that of neat PLA. The high retention of strength in the composites suggests that SBP could be a very competitive filler to other cellulosic fiber fillers. The increased tensile mechanical properties were attributed to the improved interfacial adhesion by the addition of pMDI and the enhanced mechanical interlocking owing to the better penetration of PLA into the SBP particles. The microstructure of the fracture surfaces revealed that the debonding of the SBP particles from the PLA matrix was increasingly prevented with pMDI content. Instead, the SBP particles were broken through on the fracture surfaces. Further evidence of rupture of the SBP particles was provided by the SBP particle size analysis of the fracture surfaces, using the images of SBP autofluorescence. On the other hand, the impact strength decreased with the addition of pMDI. Molecular weight change of PLA was also noted in the composites, most likely owing to thermal degradation and hydrolysis. These results

indicate that through improving the interfacial adhesion the low cost SBP as filler can result in PLA composites with properties close to that of neat PLA but with great cost reduction.

Literature Cited

(1) Jiang, L.; Wolcott, M. P.; Zhang, J. Study of biodegradable polylactide/poly(butylene adipate-*co*-terephthalate) blends. *Biomacromolecules* **2006**, *7*, 199.

(2) Zhang, J.; Jiang, L.; Zhu, L.; Jane, J.; Mungara, P. Morphology and properties of soy protein and polylactide blends. *Biomacromolecules* **2007**, *7*, 1551.

(3) Jiang, L.; Zhang, J.; Wolcott, M. P. Comparision of polylactide/nano-sized calcium carbonate and polylactide/montmorillonite composites: Reinforcing effects and toughening mechanisms. *Polymer* **2007**, *48*, 7632.

(4) Shibata, M.; Oyamada, S.; Kobayashi, S. I.; Yaginuma, D. Mechanical properties and biodegradability of green composites based on biodegradable polyesters and lyocell fabric. *J. Appl. Polym. Sci.* **2004**, *92*, 3857.

(5) Hu, R.; Lim, J. K. Fabrication and mechanical properties of completely biodegradable hemp fiber reinforced polylactic acid composites. *J. Compos. Mater.* **2007**, *41*, 1655.

(6) Garcia, M.; Garmendia, I.; Garcia, J. Influence of natural fiber type in eco-composites. *Appl. Polym. Sci.* **2008**, *107*, 2994.

(7) Shibata, M.; Ozawa, K.; Teramoto, N.; Yosomiya, R.; Takeishi, H. Biocomposites made from short abaca fiber and biodegradable polyesters. *Macromol. Mater. Eng.* **2003**, *288*, 35.

(8) Pilla, S.; Gong, S.; O'Neill, E.; Rowell, R. M.; Krzysik, A. M. Polylactide-pine wood flour composites. *Polym. Eng. Sci.* **2008**, *48*, 578.

(9) Lee, S. H.; Wang, S. Biodegradable polymers/bamboo fiber biocomposite with bio-based coupling agent. *Composites, Part A: Appl. Sci. Manuf.* **2006**, *37*, 80.

(10) Huda, M. S.; Drzal, L. T.; Misra, M.; Mohanty, A. K. Wood-fiber-reinforced poly(lactic acid) composites: Evaluation of the physicomechanical and morphological properties. *J. Appl. Polym. Sci.* **2006**, *102*, 4856.

(11) Sheldon, R. P. *Composite Polymeric Materials*; Applied Science Publisher: London, 1982; p 88.

(12) Suszkiw, J. Beets: A biodegradable bonus for earth-friendly plastics. *Agric. Res.* **2008**, *56* (3), 20.

(13) Dufresne, A.; Cavaille, J.-Y.; Vignon, M. R. Mechanical behavior of sheets prepared from sugar beet cellulose microfibrils. *J. Appl. Polym. Sci.* **1997**, *64*, 1185.

(14) Dinand, E.; Chanzy, H.; Vignon, M. R. Suspension of cellulose microfibrils from sugar beet pulp. *Food Hydrocolloids* **1999**, *13*, 275.

(15) Leitner, J.; Hinterstoisser, B.; Wastyn, M.; Keekes, J.; Gindl, W. Sugar beet cellulose nanofibril-reinforced composites. *Cellulose* **2007**, *14*, 419.

(16) Liu, L. S.; Fishman, M. L.; Hicks, K. B.; Liu, C.-K. Biodegradable composites from sugar beet pulp and poly(lactic acid). *J. Agric. Food Chem.* **2005**, *53*, 9017.

(17) Finkenstadt, V. L.; Liu, L. S.; Willett, J. L. Evaluation of poly(lactic acid) and sugar beet pulp green composites. *J. Polym. Environ.* **2007**, *15*, 1.

(18) Liu, L. S.; Finkenstadt, V. L.; Liu, C.-K.; Coffin, D. R.; Willett, J.-L.; Fishman, M.-L.; Hicks, K. B. Green composites from sugar beet pulp and poly(lactic acid): structural and mechanical characterization. *J. Biobased Mater. Bioenergy* **2007**, *1*, 323.

(19) Rouilly, A.; Jorda, J.; Rigal, L. Thermo-mechanical processing of sugar beet pulp. I. Twin-screw extrusion process. *Carbohydr. Polym.* **2006**, *66*, 81.

(20) Frazier, C. E.; Ni, J. On the occurrence of network interpenetration in the wood-isocyanate adhesive interphase. *Int. J. Adhes. Adhes.* **1998**, *18*, 81.

(21) Girones, J.; Pimenta, M. T. B.; Vilaseca, F.; de Carvalho, A. J. F.; Mutje, P.; Curvelo, A. A. S. Blocked isocyanates as coupling agents for cellulose-based composites. *Polymer* **2007**, *683*, 537.

(22) Geng, Y.; Li, K.; Simonsen, J. A combination of poly(diphenylmethane diisocyanate) and stearic anhydride as a novel compatibilizer for wood−polyethylene composites. *J. Adhes. Sci. Technol.* **2005**, *19*, 987.

(23) Harada, M.; Ohya, T.; Iida, K.; Hayashi, H.; Hirano, K.; Fukuda, H. Increased impact strength of biodegradable poly(lactic acid)/poly(butylene succinate) blend composites by using isocyanate as a reactive processing agent. *J. Appl. Polym. Sci.* **2007**, *106*, 1813.

(24) Harada, M.; Iida, K.; Okamoto, K.; Hayashi, H.; Hirano, K. Reactive compatibilization of biodegradable poly(lactic acid)/poly(ε-caprolactone) blends with reactive processing agents. *Polym. Eng. Sci.* **2008**, *48*, 1359.

(25) Ohkita, T.; Lee, S. H. Effect of aliphatic isocyanates (HDI and LDI) as coupling agents on the properties of eco-composites from biodegradable polymers and corn starch. *J. Adhes. Sci. Technol.* **2004**, *18*, 905.

(26) Aoyagi, Y.; Yamashita, K.; Doi, Y. Thermal degradation of poly((R)-3-hydroxybutyrate), poly(ε-caprolactone), and poly((S)-lactide). *Polym. Degrad. Stab.* **2002**, *76*, 53.

(27) Siparsky, G. L.; Voorhees, K. J.; Miao, F. Hydrolysis of polylactic acid (PLA) and polycaprolactone (PCL) in aqueous acetonitrile solutions: autocatalysis. *J. Environ. Polym. Degrad.* **1998**, *6*, 31.

(28) Woo, S. I.; Kim, B. O.; Jun, H. S.; Chang, H. N. Polymerization of aqueous lactic acid to prepare high molecular weight poly(lactic acid) by chain-extending with hexamethylene diisocyanate. *Polym. Bull.* **1995**, *35*, 415.

(29) Bao, S.; Daunch, W. A.; Sun, Y.; Rinaldi, P. L.; Marcinko, J. J.; Phanopoulos, C. Solid state two-dimensional NMR studies of polymeric diphenylmethane diisocyanate (PMDI) reaction in wood. *Forest Prod. J.* **2003**, *53*, 63.

(30) Reinsch, V. E.; Kelley, S. S. Crystallization of poly(hydroxybutrate-co-hydroxyvalerate) in wood fiber-reinforced composites. *J. Appl. Polym. Sci.* **1997**, *64*, 1785.

(31) Mohamed, A. A.; Finkenstadt, V. L.; Palmquist, D. E. Thermal properties of extruded/injection-molded poly(lactic acid) and biobased composites. *J. Appl. Polym. Sci.* **2008**, *107*, 898.

(32) Chen, X.; Guo, Q.; Mi, Y. Bamboo fiber-reinforced polypropylene composites: A study of the mechanical properties. *J. Appl. Polym. Sci.* **1998**, *69*, 1891.

(33) Wong, S.; Shanks, R.; Hodzic, A. Properties of poly(3-hydroxybutyric acid) composites with flax fibres modified by plasticizer absorption. *Macromol. Mater. Eng.* **2002**, *287*, 647.

(34) Oksman, K.; Clemons, C. Mechanical properties and morphology of impact modified polypropylene-wood flour composites. *J. Appl. Polym. Sci.* **1998**, *67*, 1503.

(35) Zuiderduin, W. C. J.; Westzaan, C.; Huetink, J.; Gaymans, R. J. Toughening of polypropylene with calcium carbonate particles. *Polymer* **2002**, *44*, 261.

(36) Argon, A. S.; Cohen, R. E. Toughenability of polymers. *Polymer* **2003**, *44*, 6013.

(37) Wang, H.; Sun, X.; Seib, P. Strengthening blends of poly(lactic acid) and starch with methylenediphenyl diisocyanate. *J. Appl. Polym. Sci.* **2001**, *82*, 1761.

(38) Smith, G. D. The effect of some process variables on the lap-shear strength of aspen strands uniformly coated with pMDI resin. *Wood Fiber Sci.* **2004**, *36*, 228.

Received for review June 12, 2008
Revised manuscript received September 8, 2008
Accepted September 17, 2008

IE800930J